

# **A performance-based comparison for the synthesis of Plavix (Clopidogrel) in a microreactor vs. batch reactor: From CuBr<sub>2</sub> homogeneous catalysis to heterogeneous catalysis using a Cu-based MOF (VNU-18)**

Amirreza Erfani Gahrouei <sup>a</sup>, Mohammad Kazemeini <sup>a\*</sup>, Shayan Jahangirifard <sup>a</sup>, Vahid Hosseinpour <sup>a</sup>, and Sina Pourebrahimi <sup>b\*</sup>

<sup>a</sup> *Department of Chemical and Petroleum Engineering, Sharif University of Technology, Tehran, Iran*

<sup>b</sup> *Department of Chemical and Materials Engineering, Concordia University, 7141 Sherbrooke Street West, Montréal, Quebec H4B 1R6, Canada*

\* Corresponding authors.

E-mail addresses and phone numbers of authors:

[Amirreza.erfani.g@gmail.com](mailto:Amirreza.erfani.g@gmail.com), +989136832411 (A. Erfani Gahrouei)

[kazemini@sharif.edu](mailto:kazemini@sharif.edu), +989121305309 (M. Kazemeini)

[shayan.jahangirifard@gmail.com](mailto:shayan.jahangirifard@gmail.com), +989910987096 (S. Jahangirifard)

[vahidhp@gmail.com](mailto:vahidhp@gmail.com), +989123243713 (V. Hosseinpour)

[s\\_poureb@live.concordia.ca](mailto:s_poureb@live.concordia.ca), +14384628282 (S. Pourebrahimi)

## **Abstract**

We investigated the continuous-flow synthesis of Plavix using both homogeneous and heterogeneous catalysis in a microreactor. In the homogeneous system, we employed the CuBr<sub>2</sub> catalyst, while for the heterogeneous system, we utilized a Cu-based MOF (VNU-18 metal-organic framework) catalyst. The performance of each catalytic system was evaluated based on factors such as feed flow rate, reaction temperature, catalyst loading, residence time, and solvent. An optimal Plavix production yield of 58.2% was achieved at 50 °C in 40 min under continuous-flow homogeneous catalysis using DMSO as the solvent. Moving on to heterogeneous catalysis,

we examined the performance of both batch and microreactors. The microreactor system ceased the reaction after 25 min, rendering a production yield of 42.7% at room temperature with DMF as the solvent. In contrast, the batch system yielded 50.7% after 12 h. A comparison between the performance of the flow reactors with that of the batch system reveals that the flow systems are more promising to be the future trend of processing at the industrial scale for the Plavix production than that of the batch in terms of comparable product yields yet much-lowered reaction time.

**Keywords:** *Reactor design; Continuous-flow synthesis; Metal-organic frameworks; Catalysis; Chemical reaction*

## 1. Introduction

Plavix (i.e., Clopidogrel) is an antiplatelet drug that treats cardiovascular diseases like heart attacks and strokes [1]. This chemical compound works by helping to prevent forming of harmful blood clots [2]. Bristol-Myers Squibb and Sanofi-Aventis commercially distribute this medication as Plavix, which comes in the form of 75 mg oral tablets [3]. Indeed, during the mid-2000s, this particular pharmaceutical product was considered one of the top-selling medications [4]. Studies have shown that Plavix is more effective than aspirin at preventing platelet aggregation, even at much lower doses [5]. Moreover, it has been established that the Plavix dosage of 75 mg exhibited superior efficacy compared to the aspirin dosage of 325 mg [6]. Consequently, this compound has aroused the interest of numerous teams engaged in synthetic drug research as a viable candidate for total commercial synthesis. In this regard, Khan et al. developed the molybdenum-catalyzed regio- and enantioselective amination of allylic carbonates to synthesize Plavix, achieving a production yield of up to 96% [7]. Battaglia et al. synthesized

Plavix using commercially available reagents and a quinidine-derived organocatalyst. The Knoevenagel/asymmetric epoxidation/domino ring-opening esterification (DROE) sequence generated Plavix with a 61% overall yield [8]. Li et al. synthesized Plavix through sequential I<sub>2</sub>-mediated *sp*<sup>3</sup> C–H amination and condensation of ketones with 2-aminopyridines in the presence of Na<sub>2</sub>CO<sub>3</sub> in a one-pot reaction, achieving a 57% production yield [9]. Chen et al. developed a Pd-catalyzed C–O cross-coupling of O-acyl hydroxylamines and tertiary alkyl electrophiles, resulting in the synthesis of Plavix with a 61% production yield [10].

The molecular structure of Plavix contains the amino ester functional group [11]. Traditional techniques for synthesizing compounds with amino esters typically involve the reaction of halo compounds (chemical compounds containing halogens) with amines. This reaction leads to the formation of a byproduct called halo acid [12]. In this respect, one of the most important reactions is treating the amine compound 4,5,6,7-tetrahydrothieno[3,2-c] pyridine with a bromo compound. In most cases, bromomethyl 2-bromo-2-(2-chlorophenyl) acetate reacts with the amine compound methyl 2-amino-2-(2-chlorophenyl) acetate, along with the dibromo compound 2-(2-bromoethyl) 3-(bromomethyl)thiophene and the dibromo compound 2-(2-bromoethyl)thiophene, while generating KBr as a byproduct (see Fig. 1) [11].

However, these processes involve the use of expensive and toxic reagents or result in the production of acid intermediate byproducts (e.g., HBr), necessitating quenching and neutralization. Typically, reagents like K<sub>2</sub>CO<sub>3</sub> are employed to transform these intermediate byproducts into less toxic compounds, such as KBr (the final byproduct, refer to Fig. 1). As a result, developing the green and cost-effective Plavix synthesis process is of great importance. Evans et al. conducted a study where they successfully synthesized the antiplatelet agent Plavix in a single step. They achieved an 87% product yield using affordable chemical compounds and

a standard  $\text{CuBr}_2$  homogeneous catalysis method in a batch system. The reaction involved the treatment of specific amine and bromo compounds (see Fig. 2). In the presence of  $\text{CuBr}_2$  catalyst, different types of molecules with a carbon-oxygen double bond (carbonyl substrates) can be brominated at the  $\alpha$ -position in their structure. This reaction occurs through a copper-bound enolate. As a result of this reaction, an  $\alpha$ -bromo carbonyl molecule is formed, along with two molecules of copper(I) bromide and a molecule of  $\text{HBr}$ . Moreover, the  $\alpha$ - $\text{C}=\text{O}$  functionality can be substituted with a secondary amine, leading to the formation of an  $\alpha$ -amino carbonyl compound and another molecule of  $\text{HBr}$ . To sustain the catalytic process, copper(I) bromide undergoes oxidation to form copper(II) bromide through using oxygen in the presence of  $\text{HBr}$ . The sole resultant product of this procedure is water [13].

As mentioned above, homogeneous catalysis is used in most Plavix synthesis methods. However, such catalytic systems are sensitive to several technical issues, which makes them less attractive. The majority of homogeneous catalysts exhibit toxicity and corrosiveness. Moreover, their substantial solubility in reaction mixtures produces products with relatively low quality and purity [14]. In addition, the process of neutralizing and washing the product entails the simultaneous consumption of chemical agents and substantial quantities of fresh water, rendering them economically disadvantageous. Hence, heterogeneous catalysts tend to be used due to less corrosion, easier separation, longer life, and reduced costs due to their recyclability for further synthesis cycles [15]. In this respect, Tran et al. proposed a one-step route to the antiplatelet medicine Plavix, which was formed in 61% product yield from reasonably priced commercial materials using a Cu-based MOF heterogeneous catalyst (i.e., VNU-18 metal-organic framework) in a batch system according to the following reaction (see Fig. 3). In the presence of

the copper catalyst, carbonyl compounds undergo  $\alpha$ -bromination to form  $\alpha$ -bromo carbonyls. These compounds then undergo nucleophilic substitution with N-H amines [16].

Countless chemical reactions and syntheses have been conducted within test tubes, flasks, and other containers made of glass. However, such batch synthesis is restricted to a high extent by the need for rapid and generalized high-throughput and reproducible experimental procedures. In this sense, continuous synthetic procedures can be implemented to overcome these shortcomings [17-19]. As a complementary technology to batch synthesis, continuous-flow synthesis is emerging as a powerful technology [20]. A flow reactor is capable of producing products continuously once the reaction stabilizes, making it a more suitable option for large-scale production compared to a batch reactor. The novel microreactor technology allows the development of continuous-flow processes on a lab scale with improved efficiency [21]. This technology has addressed traditional batch synthesis approaches' inherent drawbacks and challenges [22,23]. Microreactors provide several advantages over batch reactors. These advantages include higher surface-to-volume ratios, improved rates of mass and heat transfer, shorter reaction times within the reactor, cost-effectiveness, portability, reduced reagent consumption, improved reproducibility, more precise control over process parameters and safer operation [24-26].

Because of their utility in various applications in biology, chemistry, and medicine, microfluidic or lab-on-a-chip (LOC) devices have attracted interest as components of microflow systems [27]. Notably, the elevated surface-to-volume ratio of these devices improves the heat transfer rate in both highly endothermic and exothermic processes. This is achieved by preventing the formation of significant temperature gradients. Nonetheless, microflow systems

have a limited throughput that appears significant on an industrial scale. Several microfluidic devices may be utilized in parallel to continuously produce different products at an industrial scale for increased throughput to address this drawback of microreactors [28]. This method of scale-out, also known as numbering-up, enables the production of significant quantities of products without altering the chemical composition of the reaction or confronting the challenges typically linked to conventional scale-up adjustments [29].

The present study proposes a continuous-flow strategy for synthesizing Plavix in a microreactor for the first time, which has traditionally been performed via batch technology, as thoroughly discussed above. In this venue, a glass microfluidic device was fabricated as a microreactor. The glass microfluidic device's manufacturing technique is presented in the following section. Plavix's continuous-flow synthesis through both homogeneous and heterogeneous catalysis utilizing the homemade glass microreactor was investigated. In this respect, a  $\text{CuBr}_2$ -based homogeneous catalyst was used in the former process, whereas a Cu-based MOF (i.e., VNU-18 metal-organic framework) heterogeneous catalyst was first synthesized, then characterized, and ultimately utilized in the latter process. Moving forward, Plavix synthesis in the batch reactor and the continuous-flow microreactor were performed and compared under both homogeneous and heterogeneous catalysis conditions. Each catalytic system's performance was examined concerning several factors, including feed flow rate, reaction temperature, microreactor residence time, catalyst loading, and solvent type.

## **2. Experimental section**

### **2.1. Microreactor fabrication**

Fig. 4-a illustrates the microreactor pattern with a total length of 120 mm and diameter of 0.8 mm, which was fabricated by employing a laser engraving technique on soda lime glass. The step-by-step procedure for microreactor fabrication can be found in Section S1 of the Supplementary material. Fig. 4-b shows the photograph of the glass microreactor prepared in this research. As seen, it comprised two inlet ports, a T-junction, a region for performing reactions and an outlet port.

## **2.2. Materials and methods**

This section can be found in the Supplementary material (see Section S2).

## **2.3. Synthesis of the Cu-based MOF (VNU-18) heterogeneous catalyst**

The detailed procedure for the synthesis of Cu-based MOF heterogeneous catalyst is provided in the Supplementary material (see Section S3). According to the ICP-MS analysis, the final activated/dried product (163 mg) was found to contain an estimated 47.59 mg of Cu. Considering the initial use of 55.24 mg of Cu during synthesis (i.e., 210 mg of  $\text{Cu}(\text{NO}_3)_2 \cdot 3\text{H}_2\text{O}$ ), the resulting Cu utilization rate was calculated to be approximately 86.15%. This utilization rate serves as a key measure, providing insights into the effectiveness of Cu integration into the VNU-18 MOF and offering valuable information about the overall success of the synthesis process. Additionally, ICP-MS suggested a chemical formula of  $\text{C}_{35}\text{H}_{17}\text{N}_5\text{O}_{26}\text{Cu}_6$  for the synthesized VNU-18 in this work, closely matching the theoretical one reported in the literature [16]. Fig. 5 illustrates the step-by-step solvothermal synthesis procedure of the VNU-18 heterogeneous catalyst.

## **2.4. Plavix synthesis using the Cu-based MOF (VNU-18) heterogeneous catalyst and $\text{CuBr}_2$ homogeneous catalyst**

The detailed procedures for the synthesis of Plavix in the glass microreactor fabricated in this study and batch reactor using heterogenous and homogenous catalysts are provided in the Supplementary material (see Sections S4 to S7, please also see Figures S1-S4 for comparative results).

### 3. Results and discussion

#### 3.1. Characterization of the Cu-based MOF (VNU-18) heterogeneous catalyst

To characterize the physicochemical identity and crystallinity of the synthesized Cu-based MOF (i.e., VNU-18), the powder X-ray diffraction pattern (PXRD) of the activated product (see Fig. 5) was compared with that previously reported by Tran et al. [16]. In this regard, Fig. 6-a shows the PXRD pattern of the VNU-18 sample synthesized in this study in the range of  $2\theta=5$ -30 degrees. According to this analysis, peaks at  $2\theta$  angles of 7.9, 10, 12.1, 14.9, 15.5, 19.2, 20.1 and 22.1 degrees were identified, which are thoroughly consistent with the PXRD pattern of the VNU-18 synthesized by Tran et al. [16]. Moreover, the PXRD pattern of the prepared VNU-18 sample further revealed the pure phase of this crystalline material with no additional peaks related to the secondary solid phase(s) (e.g., unreacted precursors and other impurities), confirming the effectiveness of the solvent-exchange purification/activation procedure employed in this research [30].

Moving forward, the porous structure and the textural properties of the synthesized VNU-18 sample were investigated by evaluating the nitrogen ( $N_2$ ) adsorption and desorption isotherms collected at 77.4 K. Accordingly, the prepared VNU-18 sample was studied using this characterization technique, and the sample's  $N_2$  adsorption-desorption isotherms are shown in Fig. 6-b. Considering the IUPAC classifications, it was revealed that the isotherm curve obtained



for this porous material followed the typical type I isotherm with an H4-type hysteresis loop, indicating the presence of both micro-and mesopores in the porous structure of the synthesized VNU-18 sample [31-34]. In addition, the BET specific surface area and pore volume of the synthesized VNU-18 were  $720 \text{ m}^2 \text{ g}^{-1}$  and  $0.47 \text{ cm}^3 \text{ g}^{-1}$ , respectively, which closely aligns with the values reported by [16].

The FT-IR spectrum of the synthesized VNU-18 heterogeneous catalyst is presented in Fig. 6-c. The  $-\text{OH}$  functional group's stretching vibration band appeared at  $3358 \text{ cm}^{-1}$  [35]. The weak absorption bands at  $2355$  and  $2099 \text{ cm}^{-1}$  can be assigned to the stretching vibration modes of  $\text{O}-\text{C}=\text{O}$  functionalities existing in the structure of the organic ligand (i.e., 3,5-pyridinedicarboxylic acid) [36]. The absorption bands at  $1632 \text{ cm}^{-1}$  can correspond to the stretching vibration mode of  $\text{C}=\text{O}$  functionalities [35]. Besides, the strong peaks at  $1152$  and  $1095 \text{ cm}^{-1}$  can be related to the symmetric and asymmetric stretching vibrations of  $\text{C}-\text{O}$  [37]. The absorption bands at  $995$  and  $872 \text{ cm}^{-1}$  can be assigned to the  $\text{C}-\text{H}$  functionalities' symmetric and asymmetric stretching vibrations [38,39]. Also, the peaks observed at  $616$  and  $451 \text{ cm}^{-1}$  might be due to the stretching vibrations of  $\text{Cu}-\text{O}$  bonds [40]. These results further confirmed the successful formation of VNU-18.

Fig. 6-d and 6-e represent the FESEM images of the synthesized VNU-18 heterogeneous catalyst at two different magnifications. As seen from Fig. 6-d, VNU-18 possesses a highly crystalline cube-like structure with an approximate size of  $4-8 \mu\text{m}$  (the scale bar length is  $2 \mu\text{m}$ ). The particle size analysis using DLS (Fig. 6-f) revealed a relatively narrow size distribution for the VNU-18 particles with an average size ( $D$ ) of  $3.416 \mu\text{m}$ . These results are in good agreement with those obtained through the PXRD analysis. In the meantime, some defects are observable on the surfaces of the synthesized VNU-18 (see Figs. 6-d & 6-e). In fact, it is challenging to

synthesize truly perfect crystals of MOFs in practice because any slight change in reaction conditions may lead to defects/vacancies in the material [41,42].

### **3.2. Batch synthesis of Plavix under homogeneous and heterogeneous catalysis**

Batch experiments were conducted to determine the time required to achieve the maximum product yields in different catalytic conversion systems. Table 1 shows the results of Plavix synthesis in a batch reactor through homogeneous and heterogeneous catalysis. It ought to be noted that water (H<sub>2</sub>O) is the only byproduct of these catalytic reactions [13,16]. According to the data presented in this table, the reaction reached a plateau of the product completion after 12 h of duration when using the VNU-18 heterogeneous catalyst. This meant that the heterogeneous catalyst-promoted Plavix synthesis reaction in the batch reactor reached almost a halt toward a maximum yield after the abovementioned period. In the meantime, when using CuBr<sub>2</sub> homogeneous catalyst in the batch reactor, the reaction further advanced slightly after 24 h. Therefore, it is reasonable to conclude that, for all practical purposes, the reaction in the CuBr<sub>2</sub>-catalyzed Plavix synthesis batch system was finished after almost 24 h. Unlike the CuBr<sub>2</sub>-based homogeneous catalytic system, where DMSO was the most suitable reaction solvent, DMF demonstrated the optimal production yield when working under heterogeneous catalysis using VNU-18. This may be attributed to the observation that VNU-18 has displayed a higher dispersibility in DMF [16], whereas CuBr<sub>2</sub> has shown a higher solubility in DMSO than in DMF [13]. It is reiterated that the higher dispersibility of heterogeneous catalyst (or the higher solubility of homogeneous catalyst) would result in more efficient contact with reactants, thus increasing the reaction yield.

To confirm the VNU-18 catalyst's heterogeneity during batch synthesis, we conducted the Sheldon test to check for possible Cu leaching. After a 1-hour reaction at room temperature, the

filtered mixture was stirred for an additional 11 h at 300 rpm with air bubbling. Catalytic activity dropped upon catalyst removal, with a marginal 0.75% increase in Plavix production yield (see Table 1). Results suggested negligible Cu atom leaching from VNU-18 under these conditions. We calculated the turnover number (TON) and turnover frequency (TOF) for all instances of catalytic Plavix synthesis, employing both  $\text{CuBr}_2$  homogeneous and VNU-18 heterogeneous catalysts. The results, documented in Table 1, consistently revealed higher TON and TOF values in the context of heterogeneous catalysis, emphasizing its superior catalytic efficiency compared to the homogeneous synthesis of Plavix.

### **3.3. Continuous-flow synthesis of Plavix in microreactor using VNU-18 heterogeneous catalyst**

In this section, we have examined the performance of our designed microreactor under heterogeneous catalysis conditions using the synthesized VNU-18 catalyst. In order to gain a better insight into the reactor's performance, we have investigated the effects of various influential operational parameters, including feed flow rate, temperature, and catalyst loading. Additionally, we have compared the results of heterogeneous catalysis in the microreactor with those obtained in a batch reactor during the production of Plavix. Meanwhile, we investigated the recyclability of the VNU-18 catalyst across consecutive catalytic cycles.

#### **3.3.1. Effect of feed flow rate**

The flow rate plays a significant role in the performance of flow reactors [43]. It's a fact that increasing the flow rate leads to a reduction in residence time. This is especially crucial for manipulating the space-time yield, which, in turn, impacts cost savings. Residence time is defined as how long the reagents pass through the reactor [44]. Therefore, to regulate the residence time, one either changes the reagents pump speed by changing the feed flow rate or

varies the reactor length (i.e., the reactor size). Lower flow rates lead to longer residence time in the reactor, while higher flow rates lead to shorter residence time. Inadequate residence time results in incomplete reactions and low yield. On the other hand, excessive residence time results in unproductive reagent flow. Therefore, precise tuning of residence time is essential for the optimum yield of desired products [45].

In a typical experiment in this study, we explored the effects of altering the feed flow rate of the reaction mixture, which includes both the catalyst and reactants, on the product yield. The results are presented in Table 2. The solution flow rate was varied within the range of 1 to 25  $\mu\text{L min}^{-1}$ , corresponding to residence times between 41.7 to 8.3 minutes (see Table 2). Meanwhile, the air flow rate was kept at a constant value of 5  $\mu\text{L min}^{-1}$ . According to the results, by decreasing the solution flow rate from 25 to 5  $\mu\text{L min}^{-1}$ , the product yield increased from 29.9% to 42.7%. However, decreasing the flow rate from 5 to 1  $\mu\text{L min}^{-1}$  did not significantly impact the product yield. Therefore, the flow rate of 5  $\mu\text{L min}^{-1}$  corresponding to a residence time of 25 min was selected as the optimum feed flow rate in this study.

To confirm VNU-18 catalyst heterogeneity in the continuous-flow synthesis of Plavix, we performed a Sheldon test for probable Cu leaching. After a one-pass reaction at 25 °C with a feed flow rate of 25  $\mu\text{L min}^{-1}$  (i.e., the residence time of 8.3 min), we filtered the output mixture and reintroduced it to the microreactor at 5  $\mu\text{L min}^{-1}$ . Despite deliberately prolonging the residence time from 8.3 to 25 min, the Plavix production yield increased only slightly, from 29.9% to 30.2% (see Table 2). Results demonstrated minimal Cu ion leaching from VNU-18 under these conditions. A decrease in the feed flow rate led to an increase in TON while simultaneously causing a decrease in TOF as the residence time increased (see Table 2).

For a more comprehensive description of the relationship between the feed flow rate (F) and the weight of the catalyst (W) in relation to the yield of the reaction, Fig. 7 illustrates the yield of the reaction plotted against the W/F ratio. As depicted in Fig. 7, a progressive increase in the reaction yield from 29.87% to 43.12% was observed when increasing the W/F ratio from 0.22 to 5.32, respectively. Notably, the peak production yield occurred at W/F=5.32, indicating an optimal range for catalytic activity. The non-linear relationship suggested a saturation effect, signifying that higher W/F ratios enhanced the efficiency of the Plavix synthesis process up to a certain point. Specifically, the reaction yield at W/F=5.32 is only slightly higher than that at W/F=1 (43.12% vs. 42.72%), indicating a possible plateau in the Plavix production yield beyond a specific W/F ratio. This observation necessitates considerations of practical feasibility and cost-effectiveness, as further increases in the W/F ratio may result in negligible improvements or even a declining trend.

### **3.3.2. Effect of temperature**

The effect of temperature on the Plavix production yield was also investigated (see Table 3) by performing the Plavix synthesis process at three different temperatures (i.e., 25, 40, and 55 °C). In this venue, the microreactor was placed on top of a heater surface with a temperature set at the desired value (e.g., 40 °C) to adjust the reaction temperature. It was revealed that the Plavix production yield increased from 42.7% (at 25 °C) to 45.1% (at 40 °C) and 49.7% (at 55 °C). It is worth mentioning that all the reaction parameters, except for temperature, were identical to those used in Section 6 of SIF. Meanwhile, elevating the reaction temperature resulted in a concurrent increase in both TON and TOF under constant residence time conditions (refer to Table 3).

### **3.3.3. Effect of catalyst loading**

To assess the influence of catalyst loading on the Plavix production yield, we employed four different quantities of the VNU-18 catalyst, specifically 2, 4, 6, and 8 mg, in the continuous-flow microreactor. All experiments were conducted at a constant feed flow rate of  $5 \mu\text{L min}^{-1}$  for both liquid and gas phases at  $55 \text{ }^\circ\text{C}$ . The results are presented in Table 4 and depicted in Figure 8. It was observed that the Plavix production yield increased as the amount of VNU-18 catalyst was raised from 2 to 6 mg. For example, the Plavix production yield increased from 40.4% (2 mg catalyst,  $W/F=0.4$ ) to 48.6% (4 mg catalyst,  $W/F=0.8$ ) and 49.5% (6 mg catalyst,  $W/F=1.2$ ). On the other hand, a further increase in the catalyst loading to the reaction mixture (i.e., from 6 to 8 mg) reduced Plavix production yield to 43.8%. It is noteworthy that the dimension's depth of the microreactor channels was determined microscopically to be about 130 microns. Moreover, considering the bulk density of the prepared catalyst to be  $1.26 \text{ g cm}^{-3}$ , it shall be fair to say that the 8 mg loading would have been closely packed and even might have led to clogging of the microreactor channels. In other words, under the small flow rates of  $1\text{-}25 \mu\text{L min}^{-1}$  studied here, the mixing patterns might have indeed been expected to become "unfavorable" in terms of leading to higher conversions and yields of the product sought. In the meantime, the changes in TON and TOF, while maintaining a constant residence time and altering the catalyst loading amount, mirrored the observed trend in Plavix production yield (see Table 4).

Furthermore, increasing the catalyst concentration beyond the critical catalyst loading amount might have caused the aggregation of nanoparticles. Therefore, this unexpected result might have led to further unfavorable mixing of the aggregated catalyst with the reaction solution; hence, ineffective contact between the catalyst and the reactants was obtained. In the meantime, considering the negligible difference between the Plavix production yields when using 4 and 6 mg of the VNU-18 catalyst (i.e., 48.6% vs. 49.5%, respectively), 4 mg might be considered the

optimal amount of the catalyst. With the above-mentioned results, optimum conditions for the synthesis of Plavix using a heterogeneous catalyst (of this research) are provided in Table S1 in the Supplementary material of this paper.

#### **3.3.4. The recyclability of the VNU-18 heterogeneous catalyst**

To evaluate the recyclability of the VNU-18 heterogeneous catalyst in synthesizing Plavix through continuous-flow reactions in the designed microreactor, we performed the catalytic synthesis over five consecutive cycles, and the results are shown in Fig. 9. After each cycle, the catalyst underwent a detailed recycling process, encompassing filtration, thorough washing with fresh DMF (10 mL), centrifugation (three times), washing with DI water (20 mL), centrifugation (three times), and drying at 100°C under vacuum for 4 hours. The results revealed the satisfactory recyclability of the VNU-18 catalyst, showing a modest decrease in activity in Plavix production, with the yield dropping from 13.3% to 9.6% after five consecutive catalytic cycles (see Fig. 9-a). This acceptable recyclability likely arises from the catalyst's chemical and structural stability under the specific reaction conditions employed in Plavix production. In fact, the catalyst maintained structural integrity to a high extent following five cycles of catalytic conversion and recovery. This resilience in structural integrity is evident in the PXRD pattern of the VNU-18 catalyst recycled five times, demonstrating a resemblance to that of the fresh VNU-18 catalyst (see Fig. 9-b).

#### **3.3.5. Performance comparison between heterogeneous catalysis in batch and microreactor**

According to the results presented in Table 1, the Plavix production yield of 51.2% was achieved after a prolonged reaction duration of 24 h through a conventional batch reactor. However, a reasonable production yield of 42.7% (see Table 2) in a much shorter reaction time

(i.e., 25 min, see Table 2) was obtained using the microreactor designed and fabricated in the present work. In other words, a great reduction in residence time accompanied the latter compared to the former reactor type. A continuous-flow microreactor may provide easier operation and considerably shorter reaction time benefits than the conventional batch conversion system. Due to a low space velocity through the microfluidic reactors, a higher percentage of reactants do always get in contact with one another, which may lead to a higher extent of a reaction. In addition, from the controllability point of view, since the continuous system operates under a steady state, it is indeed easier to control it than a batch with unsteady behavior. Thus, the repeatability and quality of the final product are higher in the former system. Furthermore, from the point of view of increased efficiency, due to the high surface-to-volume ratio in continuous systems, the mass and heat transfer phenomena are not limiting anymore; hence, the process efficiency ought to be enhanced. From the point of view of process safety in continuous production, the level of possible automation could also be higher; thus, the contact between system operators and chemical materials is reduced. Automated microreactor systems often consist of pumps, valves, micromixers, micro-separators, sensors and control software that work together to automate and optimize the reaction processes. These systems can be programmed to perform complex reaction sequences with minimal human intervention. Batch reactors are typically larger in size and handle larger reactant volumes than microreactors. Handling smaller quantities of reactants can potentially reduce the risk associated with handling hazardous materials.

Additionally, microreactors can be used to safely conduct exothermic reactions that would be too dangerous to perform in a batch reactor. This is because the small volume of a microreactor allows the heat to be dissipated more quickly, preventing the reaction from getting out of control.



Scaling up a batch reactor involves increasing the size or volume of a single batch reactor, which can be challenging because it can lead to changes in the reaction kinetics, mixing and heat transfer. However, in microreactor systems, scaling up is achieved through a concept called numbering up or scaling out. Numbering up refers to increasing the number of individual microreactors operating in parallel to achieve a larger production capacity. This allows the generation of significant product quantities without impacting the reaction kinetics or the heat and mass transfer aspects of the process, as the reactor dimensions remain unaltered. Hence, the continuous-flow microreactor has proven to be an effective tool for optimizing the synthesis process of any material and, in particular, Plavix in the current study.

### **3.4. Continuous-flow synthesis of Plavix in microreactor using the CuBr<sub>2</sub> homogeneous catalyst**

#### **3.4.1. Effect of reaction time**

As discussed earlier, the reaction time (i.e., residence time) is a crucial component that may impact the production yield and reagent conversion. However, it's important to note that changing the feed flow rates directly influences the mixing rate of the reactants. Consequently, we adjusted the residence time by altering the microreactor length (e.g., from 1 to 2 m). It is revealed that the production yield increased remarkably with residence time increase, reaching from 34% at 20 min (1 m length) to 37% at 30 min (1.5 m length) to about 41.5% at 40 min (2 m length) at room temperature using DMSO as solvent (see Table 5). It ought to be noted that the feed flow rates of both liquid and gas phases were kept constant at 2  $\mu\text{L min}^{-1}$ . Moreover, an extension in the reaction time (i.e., microreactor tube length) resulted in an elevation of TON, accompanied by a reduction in TOF (refer to Table 5).

#### **3.4.2. Effect of temperature**

The effect of temperature on the Plavix production yield was also examined by carrying out the Plavix synthesis reaction at three different temperatures (i.e., 25, 35, and 50 °C), and the results are outlined in Table 6. Similar to the process explained in Section 3.3.2 for the effect of temperature upon the VNU-18-catalyzed continuous-flow Plavix production system, here the microreactor was also placed on top of a heater surface with a temperature set at the desired value (e.g., 35 °C) to adjust the reaction temperature. It should be noted that the time needed to reach a steady state was about 45 min. It was found that the Plavix production yield increased from 41.1% (at 25 °C) to 46.1% (at 35 °C) and 58.2% (at 50 °C). Moreover, increasing the reaction temperature led to a corresponding rise in both TON and TOF while maintaining constant residence time conditions (see Table 6).

#### **3.4.3. Effect of feed flow rate**

An increased feed flow rate may impact the microreactor's mixing rate. Hence, adjusting the microchannel length could keep the residence time constant while studying the effect of changing feed flow rates and, thus, mixing rates on the production yield. This study showed that the production yield was enhanced under higher gas and liquid feed flow rates (see Table 7). This indeed displays the role of mixing quality in this reaction. Additionally, an increase in feed flow rates resulted in a simultaneous increase in both TON and TOF under constant residence time conditions (refer to Table 7).

#### **3.4.4. Effect of solvent type**

Solvent type can also significantly influence the production of Plavix, as the solvent can affect the mass transfer rate and the solubility of reactants and catalysts in the reaction medium. Solvent type effect on the Plavix production yield using CuBr<sub>2</sub> homogeneous catalyst was investigated at 50 °C with the feed flow rates of both the liquid and gas phases adjusted to 5 μL

$\text{min}^{-1}$ . Besides, the reaction time was 40 min. The results in Table 8 illustrate that DMSO was the most suitable solvent (i.e., reaction medium) for this reaction in the microreactor designed and fabricated in this research. DMSO provided a 58.2% yield of the Plavix production. In the meantime, lowered Plavix production yields of 26.8% and 39.1% were achieved when using DMF and DMA as the reaction solvents. Optimum conditions for Plavix synthesis using a homogenous catalyst (of this investigation) are provided in the Supplementary material (see Table S2) of this paper. Meanwhile, TON and TOF exhibited a similar trend to the Plavix production yield when employing different solvents (see Table 8).

#### **4. Conclusion**

This research developed a procedure to synthesize an antiplatelet drug, Plavix (i.e., Clopidogrel), in a low-cost glass microreactor through homogeneous and heterogeneous catalysis. First, Plavix was synthesized using a Cu-based MOF (i.e., VNU-18) heterogeneous catalyst, and the performance of the microreactor was compared with that of a conventional batch reactor under the same reaction conditions. The influence of the reaction mixture flow rate, reaction temperature, and catalyst loading, as the most significant parameters on the reaction yield, was investigated. It was observed that the reaction yield was enhanced when the reaction mixture flow rate was increased up to a specific value. Beyond that specific flow rate, the reaction yield remained relatively constant. According to the results, the reaction was carried out in 25 min in the microreactor system, providing a maximum yield of 42.7%.

Meanwhile, under the same general conditions through a batch system, the maximum yield of 50.7% was achieved after a prolonged reaction time of 12 h. The residence time through the fabricated microreactor was much shorter than that of the conventional batch reactor, while a rather small difference in the product yield was observed between them. These findings strongly

support the utilization of microreactors when considering industrial production processes. Moreover, Plavix was synthesized through a continuous-flow homogeneous catalytic system. The effective parameters, such as the reactor residence time, reaction temperature, feed flow rate, and solvent type, were investigated on the Plavix production yield. It was concluded that DMSO was the most suitable solvent for this reaction to take place through the microreactor. Moreover, after 40 min, a reaction yield of 58.2% in this reactor was reached. Although this yield was about 9% lower than the batch reactor under the same reaction conditions, the 40 vs. 1440 min reaction time for the flow vs. batch reactors made the former rather promising for real-world applications.

### **Conflict of Interests**

On behalf of all authors, the corresponding authors state that there is no conflict of interest.

Supplementary data is available at:

### **References**

- [1] Pang, J., Wu, Q., Zhang, Z., et al. "Efficacy and safety of clopidogrel only vs. clopidogrel added proton pump inhibitors in the treatment of patients with coronary heart disease after percutaneous coronary intervention: a systematic review and meta-analysis", *IJC Heart Vasc.*, **23**, p. 100317 (2019).
- [2] Singh, A., Sharma, R., Chaudhary, S., et al. "Preparation and Characterization of Clopidogrel Bisulfate-hydroxypropyl- $\beta$ -Cyclodextrin Mixed Inclusion Complex for Improved Intestinal Solubility and Anti-Thrombotic Efficacy", *J. Pharm. Sci.*, **112**(1), pp. 166–181 (2023).
- [3] Cavender, M. A., Harrington, R. A., Stone, G. W., et al. "Ischemic events occur early in patients undergoing percutaneous coronary intervention and are reduced with cangrelor: findings from CHAMPION PHOENIX", *Circ.: Cardiovasc. Interventions*, **15**(1) (2022).
- [4] Saeed, A., Shahzad, D., Faisal, M., et al. "Developments in the synthesis of the antiplatelet and antithrombotic drug (S)- clopidogrel", *Chirality*, **29**(11), pp. 684–707 (2017).

- [5] Parsa-Kondelaji, M. and Mansouritorghabeh, H., "Aspirin and clopidogrel resistance; a neglected gap in stroke and cardiovascular practice in Iran: a systematic review and meta-analysis", *Thromb. J.*, **21**(1), p. 79 (2023).
- [6] Johnston, S. C., Amarenco, P., Denison, H., et al. "Ticagrelor and aspirin or aspirin alone in acute ischemic stroke or TIA", *N. Engl. J. Med.*, **383**(3), pp. 207–217 (2020).
- [7] Khan, S., Zhang, J., and Khan, A., "Molybdenum-Catalyzed Regio- and Enantioselective Amination of Allylic Carbonates: Total Synthesis of (S)-Clopidogrel", *Org. Lett.*, (2023).
- [8] Battaglia, V., Meninno, S., and Lattanzi, A., "One- Pot Catalytic Synthesis of Optically Active Drug (S)- Clopidogrel", *Eur. J. Org. Chem.*, **26**(40), p. e202300744 (2023).
- [9] Li, K., Li, Q., Shi, Q., et al. "Iodine- Mediated  $sp^3$  C–H Amination Reactions Forming  $\alpha$ -Amino Ketones/Esters and Fused Imidazoles", *Asian J. Org. Chem.*, **11**(7), p. e202200268 (2022).
- [10] Chen, J., Xu, Y., Shao, W., et al. "Pd-Catalyzed C–O Bond Formation Enabling the Synthesis of Congested N, N, O-Trisubstituted Hydroxylamines", *Org. Lett.*, **24**(45), pp. 8271–8276 (2022).
- [11] Swain, S. P., Kumar, K. N., Mhate, M., et al. "Copper (II) bromide catalysed one pot bromination and amination for the green, cost-effective synthesis of clopidogrel", *Mol. Catal.*, **522**, p. 112210 (2022).
- [12] Simić, S., Zukić, E., Schmermund, L., et al. "Shortening synthetic routes to small molecule active pharmaceutical ingredients employing biocatalytic methods", *Chem. Rev.*, **122**(1), pp. 1052–1126 (2021).
- [13] Evans, R. W., Zbieg, J. R., Zhu, S., et al. "Simple catalytic mechanism for the direct coupling of  $\alpha$ -carbonyls with functionalized amines: a one-step synthesis of plavix", *J. Am. Chem. Soc.*, **135**(43), pp. 16074–16077 (2013).
- [14] Pourebrahimi, S., Pirooz, M., Ahmadi, S., et al. "Nanoengineering of metal-based electrocatalysts for carbon dioxide (CO<sub>2</sub>) reduction: A critical review", *Mater. Today Phys.*, **38**, p. 101250 (2023).
- [15] Cui, X., Li, W., Ryabchuk, P., et al. "Bridging homogeneous and heterogeneous catalysis by heterogeneous single-metal-site catalysts", *Nat. Catal.*, **1**(6), pp. 385–397 (2018).
- [16] Tran, T. V., Le, H. T., Ha, H. Q., et al. "A five coordination Cu (ii) cluster-based MOF and its application in the synthesis of pharmaceuticals via  $sp^3$  C–H/N–H oxidative coupling", *Catal. Sci. Technol.*, **7**(16), pp. 3453–3458 (2017).

- [17] Yoo, W.-J., Ishitani, H., Saito, Y., et al. "Reworking organic synthesis for the modern age: Synthetic strategies based on continuous-flow addition and condensation reactions with heterogeneous catalysts", *J. Org. Chem.*, **85**(8), pp. 5132–5145 (2020).
- [18] Breen, C. P., Nambiar, A. M., Jamison, T. F., et al. "Ready, set, flow! Automated continuous synthesis and optimization", *Trends Chem.*, **3**(5), pp. 373–386 (2021).
- [19] Guan, F., Blacker, A. J., Hall, B., et al. "High-pressure asymmetric hydrogenation in a customized flow reactor and its application in multi-step flow synthesis of chiral drugs", *J. Flow Chem.*, **11**, pp. 763–772 (2021).
- [20] Noel, L., Capaldo, L., and Wen, Z., "A field guide to flow chemistry for synthetic organic chemists", *Chem. Sci.*, **14**(16), pp. 4230–4247 (2023).
- [21] Mlakić, M., Rajič, L., Ljubić, A., et al. "Synthesis of new heterocyclic resveratrol analogues in milli- and microreactors: Intensification of the Wittig reaction", *J. Flow Chem.*, **12**(4), pp. 429–440 (2022).
- [22] Akwi, F. M. and Watts, P., "Continuous flow chemistry: where are we now? Recent applications, challenges and limitations", *Chem. Commun.*, **54**(99), pp. 13894–13928 (2018).
- [23] Burange, A. S., Osman, S. M., and Luque, R., "Understanding flow chemistry for the production of active pharmaceutical ingredients", *iScience*, **25**(3), p. 103892 (2022).
- [24] Luo, F., Lei, L., Cheng, Z., et al. "Magnet-actuated microfluidic reactors with controllable Fe-based amorphous microspheres for tetracycline degradation", *J. Flow Chem.*, **12**(3), pp. 297–305 (2022).
- [25] Yang, L., Sun, Y., and Zhang, L., "Microreactor Technology: Identifying Focus Fields and Emerging Trends by Using CiteSpace II", *ChemPlusChem*, **88**(1), p. e202200349 (2023).
- [26] Myachin, I. V. and Kononov, L. O., "Mixer Design and Flow Rate as Critical Variables in Flow Chemistry Affecting the Outcome of a Chemical Reaction: A Review", *Inventions*, **8**(5), p. 128 (2023).
- [27] Bogdan, A. R. and Dombrowski, A. W., "Emerging trends in flow chemistry and applications to the pharmaceutical industry", *J. Med. Chem.*, **62**(14), pp. 6422–6468 (2019).
- [28] Liu, Y., Chen, G., and Yue, J., "Manipulation of gas-liquid-liquid systems in continuous flow microreactors for efficient reaction processes", *J. Flow Chem.*, **10**, pp. 103–121 (2020).
- [29] Domokos, A., Nagy, B., Szilagyi, B., et al. "Integrated continuous pharmaceutical technologies—A review", *Org. Process Res. Dev.*, **25**(4), pp. 721–739 (2021).

- [30] Pourebrahimi, S., Kazemeini, M., and Vafajoo, L., "Embedding graphene nanoplates into MIL-101 (Cr) pores: synthesis, characterization, and CO<sub>2</sub> adsorption studies", *Ind. Eng. Chem. Res.*, **56**(14), pp. 3895–3904 (2017).
- [31] Pourebrahimi, S., Pirooz, M., De Visscher, A., et al. "Highly efficient and reversible iodine capture utilizing amorphous conjugated covalent triazine-based porous polymers: Experimental and computational studies", *J. Environ. Chem. Eng.*, **10**(3), p. 107805 (2022).
- [32] Pourebrahimi, S. and Pirooz, M., "Synthesis of a novel freestanding conjugated triazine-based microporous membrane through superacid-catalyzed polymerization for superior CO<sub>2</sub> separation", *Chem. Eng. J. Adv.*, **11**, p. 100315 (2022).
- [33] Pourebrahimi, S., Kazemeini, M., Zaroudi, M., et al. "Methane adsorption on carbonaceous microporous materials prepared from cellulose and lignin: Equilibrium and kinetic studies", *Sci. Iran.*, **25**(6), pp. 3368–3380 (2018).
- [34] Berijani, K., Morsali, A., and Garcia, H., "Synthetic strategies to obtain MOFs and related solids with multimodal pores", *Microporous Mesoporous Mater.*, **349**, p. 112410 (2023).
- [35] Pourebrahimi, S., Kazemeini, M., Babakhani, E. G., et al. "Removal of the CO<sub>2</sub> from flue gas utilizing hybrid composite adsorbent MIL-53 (Al)/GNP metal-organic framework", *Microporous Mesoporous Mater.*, **218**, pp. 144–152 (2015).
- [36] Karmakar, G., Tyagi, A., Wadawale, A., et al. "A 2D Cu(ii) coordination polymer constructed with 2, 5-pyridinedicarboxylic acid linker: synthesis, structural analysis and its selective transformation into Cu and CuO nanoparticles", *New J. Chem.*, **47**(30), pp. 14297–14305 (2023).
- [37] Vakili, M., Gholami, F., Zwain, H. M., et al. "Removal of GenX by APTES functionalized diepoxyoctane cross-linked chitosan beads", *J. Environ. Chem. Eng.*, **11**(5), p. 110539 (2023).
- [38] Pourebrahimi, S. and Pirooz, M., "Reversible iodine vapor capture using bipyridine-based covalent triazine framework: Experimental and computational investigations", *Chem. Eng. J. Adv.*, **8**, p. 100150 (2021).
- [39] Pourebrahimi, S., Pirooz, M., Kazemeini, M., et al. "Synthesis, characterization, and gas (SO<sub>2</sub>, CO<sub>2</sub>, NO<sub>2</sub>, CH<sub>4</sub>, CO, NO, and N<sub>2</sub>) adsorption properties of the CTF-1 covalent triazine framework-based porous polymer: experimental and DFT studies", *J. Porous Mater.*, (2024).
- [40] Gao, P., Sun, X.-Y., Liu, B., et al. "Cu MOF-based catalytic sensing for formaldehyde", *J. Mater. Chem. C*, **6**(30), pp. 8105–8114 (2018).
- [41] Shan, Y., Zhang, G., Shi, Y., et al. "Synthesis and catalytic application of defective MOF materials", *Cell Rep. Phys. Sci.*, **4**(3), p. 101301 (2023).

[42] Pourebrahimi, S. and Kazemeini, M., "A kinetic study of facile fabrication of MIL-101 (Cr) metal-organic framework: Effect of synthetic method", *Inorg. Chim. Acta*, **471**, pp. 513–520 (2018).

[43] Liao, J., Zhang, S., Wang, Z., et al. "Transition-metal catalyzed asymmetric reactions under continuous flow from 2015 to early 2020", *Green Synth. Catal.*, **1**(2), pp. 121–133 (2020).

[44] Tamtaji, M. and Kazemeini, M., "Optimization of Photooxygenation of Dihydroartemisinin Acid in a Continuous Micro-reactor utilizing Physically Immobilized Methylene Blue on Polystyrene Micro-particles", *Chem. Eng. Trans.*, **88**, pp. 1327–1332 (2021).

[45] Zeibi Shirejini, S. and Mohammadi, A., "Halogen–lithium exchange reaction using an integrated glass microfluidic device: an optimized synthetic approach", *Org. Process Res. Dev.*, **21**(3), pp. 292–303 (2017).

### List of Figure Captions

**Fig. 1.** A two-step synthesis of Plavix through the  $K_2CO_3$ -based homogeneous catalysis at batch reactor [12].

**Fig. 2.** Schematic representation of the one-step synthesis of Plavix using  $CuBr_2$ -based homogeneous catalysis in a batch reactor as proposed by Evans et al. [13].

**Fig. 3.** Schematic representation of the one-step synthesis of Plavix through the heterogeneous catalysis using a Cu-based MOF (i.e., VNU-18 metal-organic framework) through a batch reactor by Tran et al. [16].

**Fig. 4.** The designed microreactor pattern (a) and the glass microreactor fabricated in this work (b).

**Fig. 5.** The step-by-step solvothermal synthesis procedure of the VNU-18 heterogeneous catalyst at 100 °C for 24 h.

**Fig. 6.** The characterization results of the Cu-based MOF (i.e., VNU-18 metal-organic framework) heterogeneous catalyst prepared in this research through the solvothermal synthetic method. (a) The



PXRD pattern of the fully dried VNU-18 sample, (b) the N<sub>2</sub> adsorption-desorption isotherms collected at 77.4 K on the activated VNU-18 sample, (c) the FT-IR spectrum of the synthesized VNU-18 collected using KBr beads, and the FESEM images of the synthesized VNU-18 with the magnification of 2 μm (d) and 200 nm (e), and (f) particle size distribution (PSD) of VNU-18.

**Fig. 7.** Effect of W/F ratio upon the reaction yield producing Plavix at 25 °C.

**Fig. 8.** Effect of W/F on yield of reaction at 55 °C.

**Fig. 9.** (a) The Plavix production yields using the VNU-18 catalyst recycled up to 5 consecutive cycles and (b) the PXRD patterns of the fresh VNU-18 catalyst and that of after 5 consecutive catalytic cycles. The reaction took place in the microreactor at 25 °C with the air and feed flow rates kept constant at 5 and 15 μL min<sup>-1</sup>, respectively.

### List of Table Captions

**Table 1.** Effect of reaction time on the Plavix production yield through homogeneous and heterogeneous catalysis in the batch reactor used in this work. For detailed experimental procedures, see Sections 4 and 5 of SIF.

**Table 2.** Continuous-flow synthesis of Plavix in the glass microreactor using the VNU-18 heterogeneous catalyst at different feed (solution mixture) flow rates at 25 °C. The total effective volume of the glass microreactor was 250 μL. The air feed flow rate was kept constant at 5 μL min<sup>-1</sup>. For detailed experimental procedures, see Section 6 of SIF.

**Table 3.** Temperature effect on the Plavix production yield using the VNU-18 heterogeneous catalyst in the glass microreactor in this study. The air and feed flow rates were both kept constant at 5 μL min<sup>-1</sup> (i.e., the residence time of 25 min).

**Table 4.** Catalyst loading effect on the Plavix production yield using the VNU-18 heterogeneous catalyst in the glass microreactor at 55 °C in this research. The air and feed flow rates were both kept constant at 5 μL min<sup>-1</sup> (i.e., the residence time of 25 min).

**Table 5.** Reaction time effect on the Plavix production yield using the CuBr<sub>2</sub> homogeneous catalyst in the glass microreactor at room temperature.

**Table 6.** Temperature effect on the Plavix production yield using the CuBr<sub>2</sub> homogeneous catalyst in the glass microreactor. The microreactor length was 2 m (i.e., the residence time was 40 min). The feed flow rates of both the liquid and gas phases were kept constant at 2 μL min<sup>-1</sup>.

**Table 7.** Feed flow rate effect (i.e., mixing effect) on the Plavix production yield using the CuBr<sub>2</sub> homogeneous catalyst in the glass microreactor at 50 °C. The reaction time was 20 min.

**Table 8.** Solvent effect on the Plavix production yield using the CuBr<sub>2</sub> homogeneous catalyst in the glass microreactor at 50 °C. The microreactor length was 2 m (i.e., the residence time was 40 min). The feed flow rates of both the liquid and gas phases were kept constant at 2 μL min<sup>-1</sup>.

### Figures

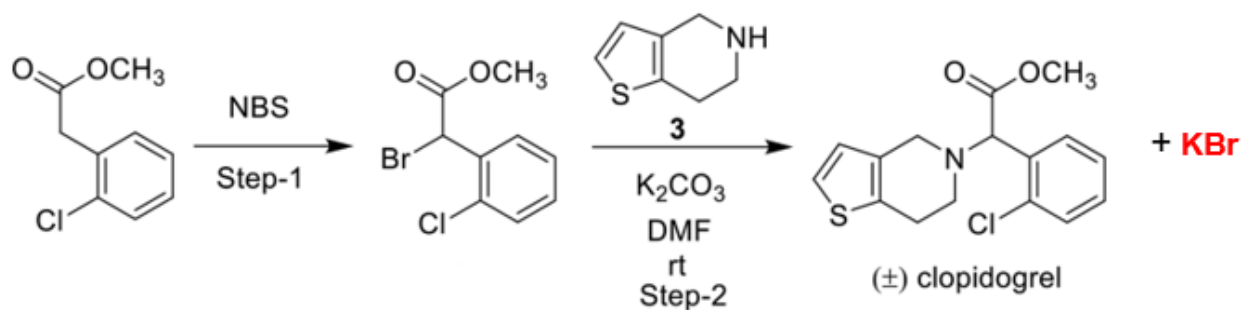


**Fig. 1.**

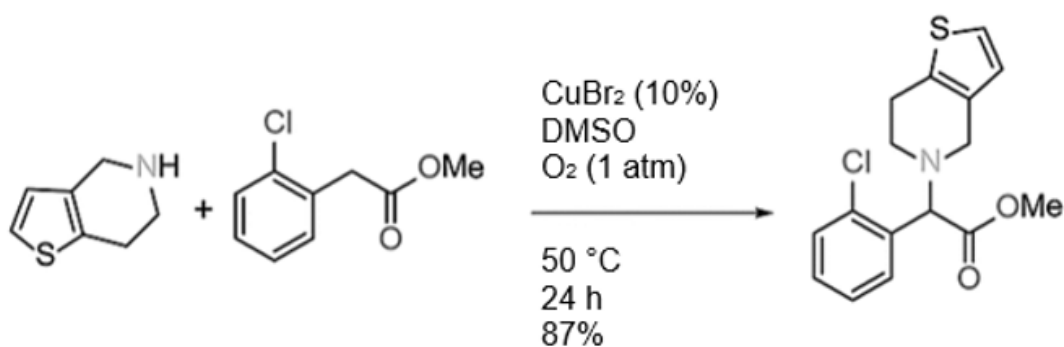


Fig. 2.

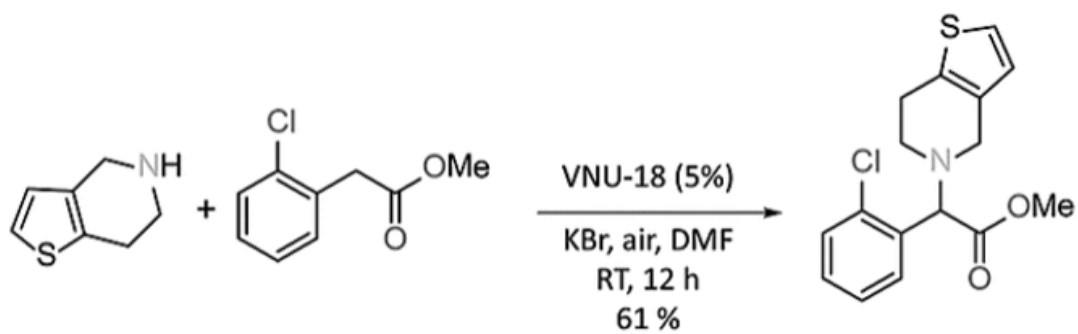
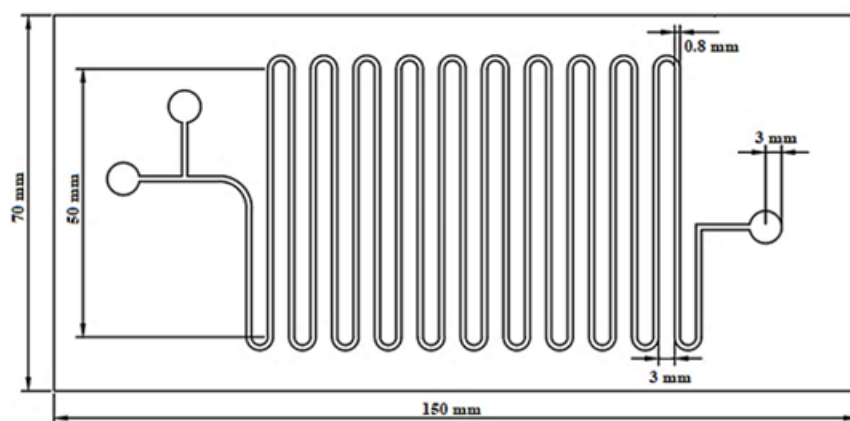
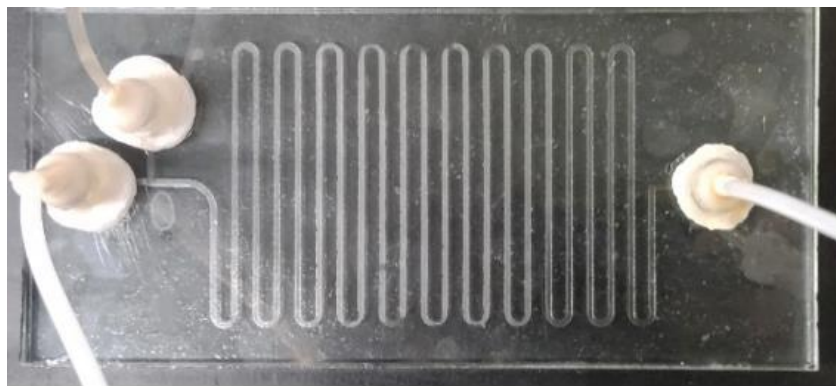


Fig. 3.



(a)



(b)

Fig. 4.

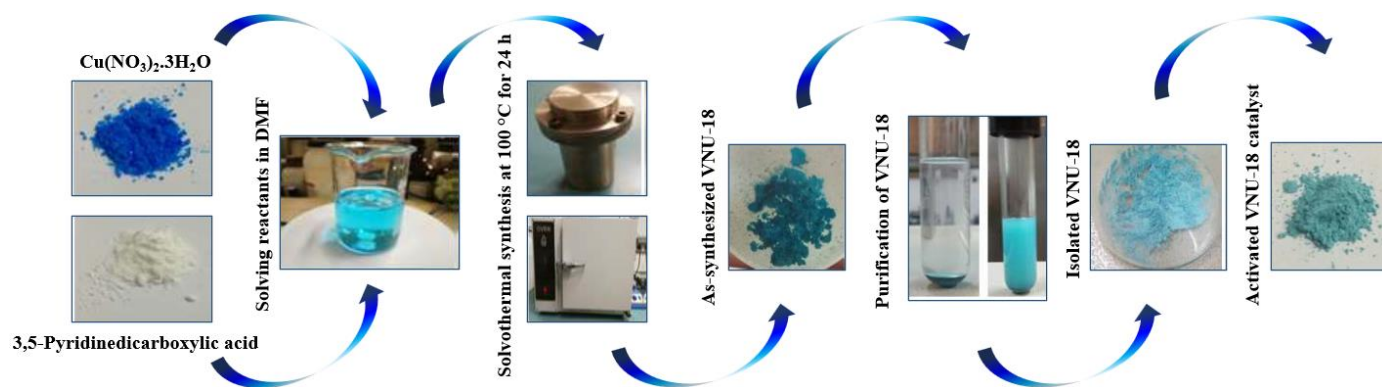
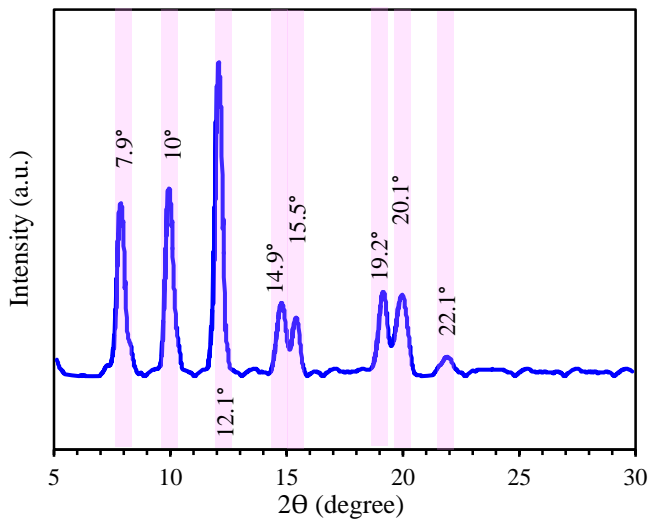
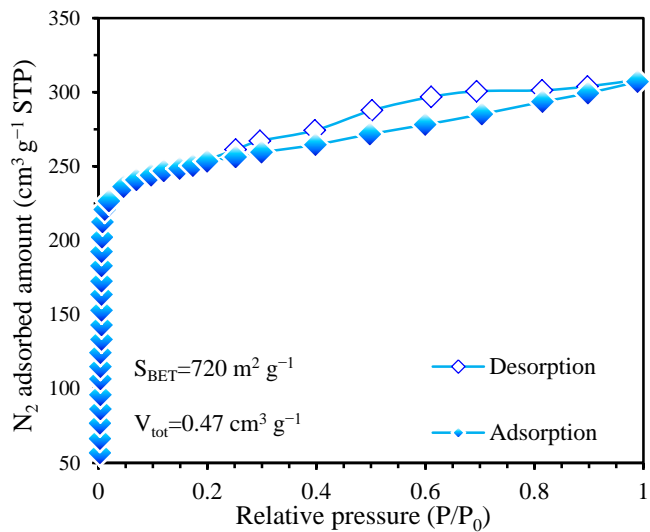


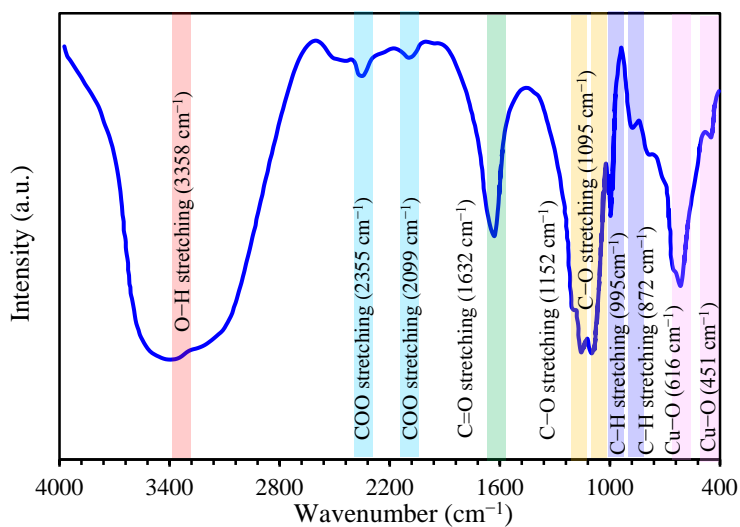
Fig. 5.



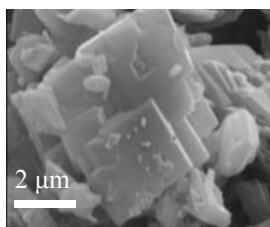
(a)



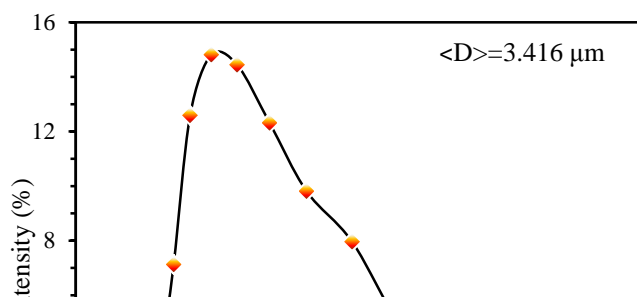
(b)

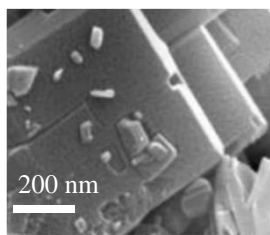


(c)



(d)





(e)

**Fig. 6.**

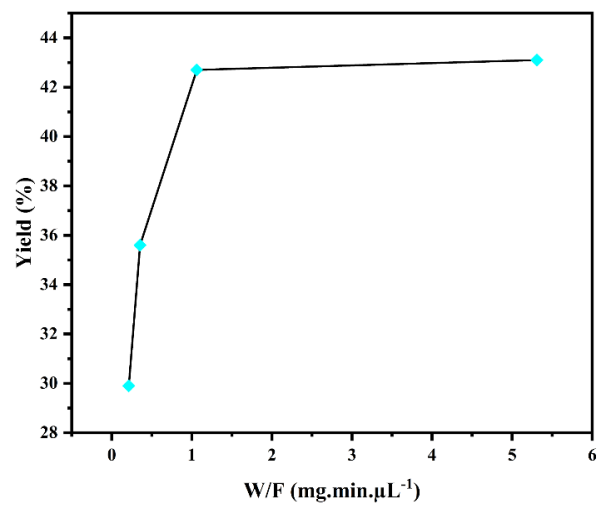


**Fig. 7.**

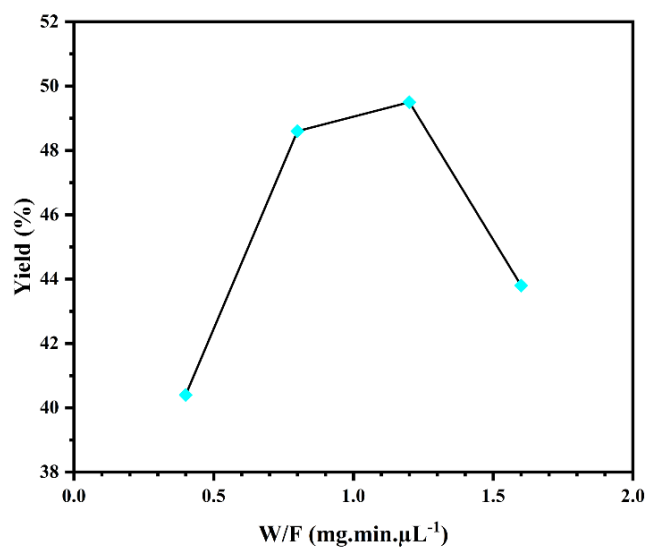


**Fig. 8.**

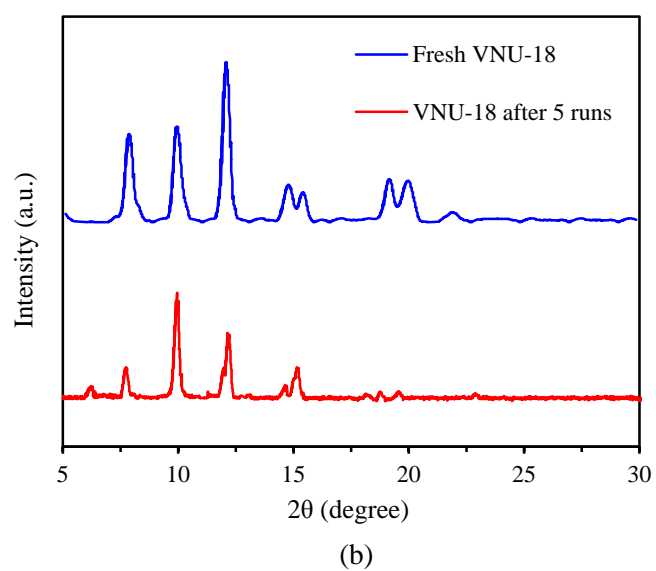
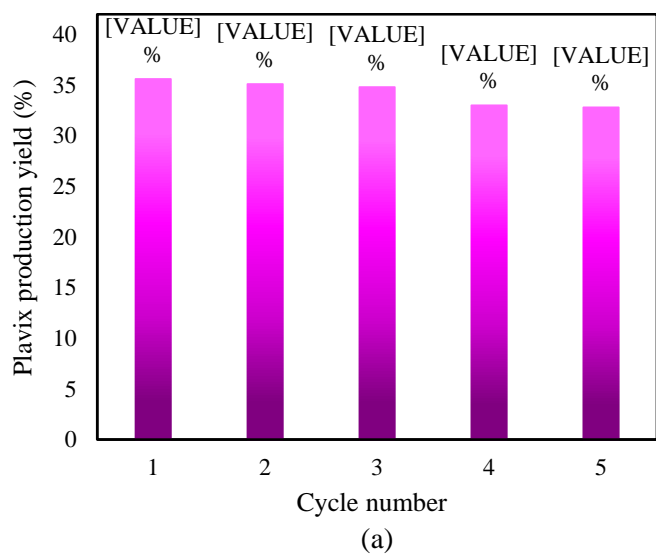


**Fig. 9.**

## Tables

**Table 1.**

Catalyst	Temperature	Solvent	Reaction time (h)	Product yield (%)	TON <sup>a</sup>	TOF <sup>b</sup> (min <sup>-1</sup> )
----------	-------------	---------	----------------------	----------------------	------------------	--

VNU-18 (Heterogeneous catalysis)	r.t.	DMF	1	13.3	26.6	0.443
			12	50.7	101.4	0.141
			1+11	13.4 <sup>c</sup>	–	–
			24	51.2	102.4	0.071
CuBr <sub>2</sub> (Homogeneous catalysis)	50 °C	DMSO	1	22.1	4.9	0.082
			12	56	12.5	0.017
			24	67.2	14.9	0.010
			36	67.9	15.0	0.007

<sup>a</sup> Turnover number of the catalyst. <sup>b</sup> Turnover frequency of the catalyst. <sup>c</sup> The Plavix production yield determined through the Sheldon test for the VNU-18 catalyst under batch synthesis conditions following the removal of the catalyst from the reaction solution after 1 h.

**Table 2.**

Feed (solution mixture) flow rate ( $\mu\text{L min}^{-1}$ )	Residence time (min)	Product yield (%)	TON	TOF ( $\text{min}^{-1}$ )
25	8.3	29.9	59.8	7.204
15	12.5	35.6	71.2	5.696
5	25	42.7	85.4	3.416
1	41.7	43.1	86.2	2.067
5	8.3+25	30.2 <sup>a</sup>	–	–

<sup>a</sup> The Plavix production yield determined through the Sheldon test for the VNU-18 catalyst under the continuous-flow synthesis conditions following the removal of the catalyst from the reaction solution after 8.3 min.

**Table 3.**



<b>Temperature</b>	<b>Product yield</b>	<b>TON</b>	<b>TOF</b>
(°C)	(%)		(min <sup>-1</sup> )
25	42.7	85.4	3.416
40	45.1	90.2	3.608
55	49.7	99.4	3.976

**Table 4.**

<b>Catalyst loading amount (mg)</b>	<b>Product yield (%)</b>	<b>TON</b>	<b>TOF (min<sup>-1</sup>)</b>
2	40.4	80.8	3.232
4	48.6	97.2	3.888
6	49.5	99.0	3.960
8	43.8	87.6	3.504

**Table 5.**

<b>Reactor length (m)</b>	<b>Reaction time (min)</b>	<b>Product yield (%)</b>	<b>TON</b>	<b>TOF (min<sup>-1</sup>)</b>
1	20	34	7.574	0.379
1.5	30	37	8.243	0.275
2	40	41.5	9.245	0.231

**Table 6.**

<b>Temperature</b>	<b>Product yield</b>	<b>TON</b>	<b>TOF</b>
--------------------	----------------------	------------	------------

(°C)	(%)	(min <sup>-1</sup> )	
25	41.1	9.156	0.229
35	46.1	10.270	0.257
50	58.2	12.966	0.324

**Table 7.**

Liquid phase flow rate (μL min <sup>-1</sup> )	Gas phase flow rate (μL min <sup>-1</sup> )	Product yield (%)	TON	TOF (min <sup>-1</sup> )
2	2	34.1	7.597	0.380
3	3	35.6	7.931	0.397
4	4	38.2	8.510	0.426

**Table 8.**

Solvent	Product yield (%)	TON	TOF (min <sup>-1</sup> )
DMSO	58.2	12.966	0.324
DMF	26.8	5.970	0.149
DMA	39.1	8.711	0.218

### Biographies

**Amirreza Erfani Gahrouei** received his BSc degree in Chemical Engineering from Petroleum University of Technology, Abadan, Iran in 2019. Then he obtained his MSc degree from Sharif University of Technology, Tehran, Iran in 2022. His research interests include heterogenous catalysis, microfluidics and chemical reaction engineering.

**Mohammad Kazemeini** received his B.E. degree from the Univ. of Minnesota at Minneapolis USA on 1984. Then he graduated with an M.S. degree from the Univ. of Virginia at Charlottesville, USA on 1986. Finally, he received his PhD degree from the Univ. of Illinois at Chicago, USA on 1990. Currently, he is a faculty member at the Chemical and Petroleum Engineering Dept. at the Sharif University holding a distinguished Professor Rank. His current research interests include; preparation, characterization and physiochemical evaluations as well as; mathematical modelling of chemical and physical kinetics of regular, Core-Shell and Magnetic catalysts. Furthermore, Alumina, Carbons (*i.e.*; CNTs, Graphene Oxide and carbon Nano-Fibers), Zeolites and MOF supported catalysts and sorbents are being closely worked upon. Moreover, designing and fabrication as well as investigating performance of microreactors and microfluidic systems applied to catalytic HDS and ODS (*i.e.*; Hydro- and Oxidative-Desulfurization) as well as; photocatalytic and catalytic API (*i.e.*; activated pharmaceutical ingredients) and organic as well as pharmaceutical pollutant materials' removal are of close interests.

**Shayan Jahangirifard** completed his MSc in Chemical Engineering from Sharif University of Technology, Tehran, Iran in 2022. His research interests are in the field of continuous-flow reactors, microfluidics, and synthesis of APIs.

**Vahid Hosseinpour** received his Bachelor's degree in chemical engineering from Shiraz University in 2007. Subsequently, he completed his M.Sc. in Chemical Engineering, specializing in Thermo-Kinetics and Catalysis at Sharif University of Technology on 2010. His research during this period primarily focused upon the kinetics study of homogeneous reactions. On 2020, he obtained his Ph.D. in chemical engineering from Sharif University of Technology. His doctoral thesis centered on the design, fabrication, and application of microfluidic devices for

catalytic conversion of hydrocarbons. Presently, he serves as an R&D member in a Gas company, concurrently continuing his research at Sharif University of Technology. His current focus involves exploring the application of microfluidic devices in healthcare and the synthesis of Active Pharmaceutical Ingredients (API). His diverse research interests encompass homogeneous and heterogeneous catalysis, kinetics studies, catalytic synthesis, Computational Fluid Dynamics, microfluidic devices, API synthesis in flow reactors, Lab-on-Chip technologies, and the application of microreactors for energy and catalytic processes.

**Sina Pourebrahimi** holds a Master's degree in Chemical Engineering, specializing in the fields of Thermo-Kinetics and Catalysis, from Sharif University of Technology in Iran. He earned his Doctoral degree in Chemical Engineering from Concordia University, Canada in 2023. His expertise and research interests are adsorption, heterogeneous catalysis, environmental chemistry and engineering, and computational chemistry.